

Implosion Simulation by Hydro Code Coupled with Laser Absorption using New Raytrace Algorithm^{*)}

Takumi YANAGAWA, Hitoshi SAKAGAMI¹⁾, Atsushi SUNAHARA²⁾ and Hideo NAGATOMO³⁾

Nagoya University, Chikusa-ku, Nagoya 464-8602, Japan

¹⁾*National Institute for Fusion Science, Oroshi-cho, Toki 509-5292, Japan*

²⁾*Institute for Laser Technology, Yamadaoka, Suita 565-0871, Japan*

³⁾*Institute of Laser Engineering, Osaka University, Yamadaoka, Suita 565-0871, Japan*

(Received 10 December 2013 / Accepted 3 May 2014)

The calculation of the laser absorption is very important for implosion simulations to capture precisely its dynamics. In many implosion simulations, the laser absorption is computed by the use of ray tracing. However, the conventional ray tracing method has the problem that it generates a non-physical absorption distribution because it represents a laser beam by a finite number of rays. Such a non-physical distribution on the target surface could be numerical perturbations that grow drastically due to Rayleigh-Taylor instability. An enormous number of rays are required to avoid such a non-physical distribution. This results in high computational costs. Thus, we have developed a new method of ray tracing that essentially generates no non-physical absorption distribution. In the new algorithm, rays are inversely traced from grid points unlike the conventional method. This paper presents the new algorithm and a preliminary implosion simulation where the pressure perturbation due to the non-uniformity of the irradiation is computed by the use of this new ray tracing.

© 2014 The Japan Society of Plasma Science and Nuclear Fusion Research

Keywords: inertial confinement fusion, implosion simulation, laser plasma interaction, ray tracing, hydrodynamics

DOI: 10.1585/pfr.9.3404090

1. Introduction

In laser fusion, a fuel capsule is imploded by the irradiation of high-intensity lasers from all directions. The fuel is compressed to 1000 times its solid density and the temperature is raised to so high that thermal nuclear fusion can occur [1]. Uniformity of irradiation is one of the most important issues to efficiently implode the fuel. In general, the ablation surface and the fuel-shell contact interface of the imploding target are Rayleigh-Taylor unstable [2–4]. Thus, perturbations on the target surface induced by the non-uniformity of the irradiation grow drastically, which degrades the implosion performance [5]. Therefore, it is very important to estimate the effect of the uniformity of the irradiation on the implosion performance by simulations. In implosion simulations, ray tracing is often used to calculate the interaction of the laser with matter. Accuracy is very important to estimate precisely the effect of the non-uniformity of the irradiation.

Sec. 2 of this paper describes the conventional ray treatment and its problem, whereas Sec. 3 presents a new algorithm that overcomes thus problem of the conventional method. Sec. 4 shows a preliminary implosion simulation with the new method applied.

2. Conventional Method

In implosion simulations, the target is assumed to be plasma, and the typical time and space scales of the plasma allow treatment of the laser light by geometrical optics [6–10]. In geometrical optics, the light is represented as a ray and the ray's position \mathbf{x} is represented by,

$$\frac{d^2\mathbf{x}}{dt^2} = -\frac{c^2}{2}\nabla\left(\frac{\rho}{\rho_c}\right), \quad (1)$$

where c , ρ and ρ_c are the light speed, mass density and critical density of plasma, respectively [6]. In a typical hydro simulation, field variables like ρ are frozen in the calculation of the ray equation. The laser light is divided into multiple beamlets and each beamlet is treated as a ray. The trajectory of each ray is obtained by solving Eq. (1) for each ray, where the initial values are defined by the position and direction of the incident laser. The light intensity of each beamlet along the trajectory is calculated from the following equation.

$$\frac{dI}{dx} = -\kappa I, \quad (2)$$

where κ is the absorption coefficient. In ablation plasma, the absorption process is assumed to be inverse bremsstrahlung and the absorption coefficient is represented by

$$\kappa = \frac{25z}{\lambda_L^2 T_e^{1.5}} \frac{(\rho/\rho_{cr})^2}{\sqrt{1 - (\rho/\rho_{cr})}}, \quad (3)$$

author's e-mail: yanagawa.takumi@nifs.ac.jp

^{*)} This article is based on the presentation at the 23rd International Toki Conference (ITC23).

where κ , z , λ_L , T_e , ρ and ρ_{cr} are the absorption coefficient in cm, charge number, laser wave length in μm , electron temperature in keV, mass density and critical density of plasma, respectively [1]. The absorbed energy of the beamlet is deposited on the plasma.

This scheme has a problem that generates a non-physical energy distribution when the number of rays is not sufficiently given (e.g.: an appendix of [10]). Figure 1 illustrates rays passing through each mesh. The color of the mesh represents the number of rays in the mesh. The energy deposited on the (i, j) mesh is contributed by two rays compared to one ray for the $(i + 1, j)$ mesh. This difference in the number of rays is directly reflected in the distribution of energy deposited on the plasma.

An example of the non-physical distribution that appeared in this conventional method is shown in Fig. 2. Figure 2(a) is the density profile with ray trajectories. The plasma profile has a 20- μm scale length that is assumed as typical for ablation plasma. The region inside the circle formed by the dotted line is the area that exceeds the critical density. Figure 2(b) is the distribution of energy deposited on plasma computed with 100 rays, and (c) with 10,000 rays, respectively. The number of grid points is 100×100 and one mesh equals one μm . The laser has a diameter of 80 μm and its normal incident from the right side. The spatial profile of the laser assumes a uniform distribution. It has been found that the case involving the 100 rays cannot fully resolve the laser beam, and therefore, the energy distribution deposited in the plasma re-

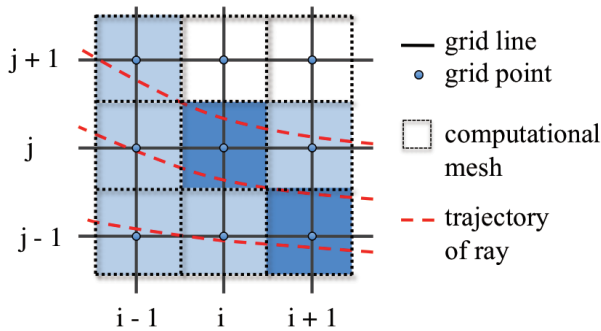


Fig. 1 A schematic diagram of ray trajectories.

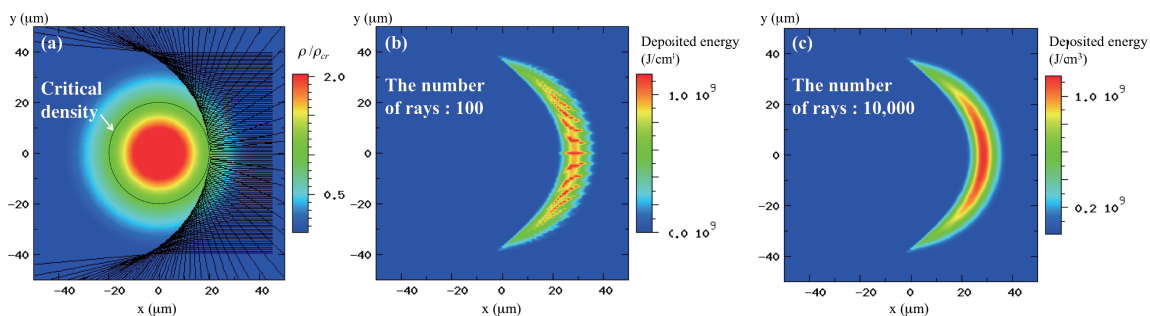


Fig. 2 (a) Density profile with ray trajectories. The laser is incident from the right side. (b) and (c) show the energy distribution deposited in this density profile with 100 rays and 10,000 rays, respectively.

sults in the non-physical distribution. This would become a numerical perturbation, which is drastically enhanced by Rayleigh-Taylor instability. This problem is associated with the number of rays and is an essential problem. To avoid the non-physical result, a vast number of rays are required. In the example of 10,000 rays, the energy distribution is sufficiently smooth. The required number of rays to avoid non-physical distribution depends on the plasma, laser and mesh size. In the case of a uniform density profile along one axis, we have estimated the required number of rays passing through one mesh to be more than 100. However, in arbitrary profiles, it is very difficult to determine the exact criterion for the number of rays. To overcome this problem, we have developed a new algorithm that essentially does not generate a non-physical result due to the number of rays.

3. Algorithm of the New Method

The new algorithm begins with searching rays that just pass through the grid point of each mesh. Using such a ray and its trajectory, the exact light intensity at the each grid point is obtained from Eq. (2). Once the light intensity at all grid points has been obtained, the distribution of the deposited energy per unit volume is defined by multiplying the light intensity by the absorption coefficient for each grid point.

However, it is quite difficult to find such a ray from the conventional ray tracing calculation. This algorithm therefore has applied an inverse ray tracing method. In this method, the ray is shot from a grid point with a certain velocity $|v|$ and angle θ . Then, the exact $|v|$ and θ required so that the ray can arrive at the area of the incident laser and the velocity is parallel to the incident direction are searched as shown in Fig. 3. As for the $|v|$, it can be defined from the following condition like the conservation law that is derived from Eq. (1):

$$\frac{1}{2} |v|^2 + \frac{1}{2} c^2 \left(\frac{\rho}{\rho_{cr}} \right) = \frac{1}{2} |v_0|^2 + \frac{1}{2} c^2 \left(\frac{\rho_0}{\rho_{cr}} \right), \quad (4)$$

where $|v_0|$ and ρ_0 are the velocity of the ray and the plasma density at the incident area of the laser, respectively. In

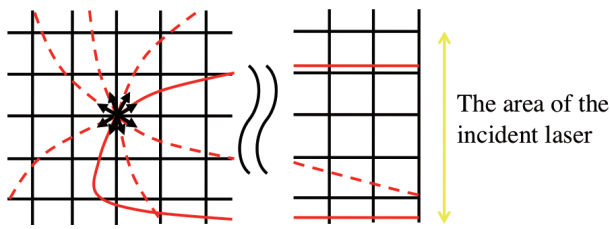


Fig. 3 A schematic diagram of inversely traced rays. The red solid lines are the exact rays that satisfy the incident condition. The laser is normal incident from the area in the yellow double-headed arrow.

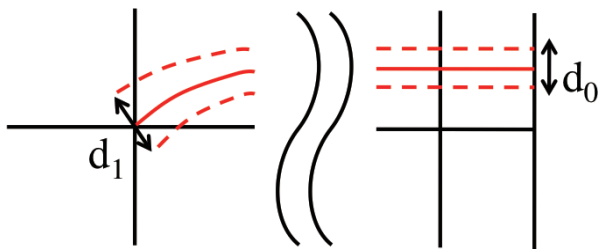


Fig. 4 A schematic diagram of the subsidiary rays. The red solid line is a main ray shot from the grid point that satisfies the incident condition. The red dashed lines indicate the subsidiary rays. d_0 and d_1 are the width of the subsidiary rays at the incident point and the grid point.

usual cases, $|v_0|$ is c and ρ_0 is 0 since the incident laser is set outside the simulation box. As for the θ , it is determined by iteration. The direction of the ray at the simulation boundary can be obtained for θ by inverse ray tracing. The direction at the boundary is considered to be the direction at the incident area because the ray travels straight in the region outside the boundary. Here we define $P(\theta)$ as the dot product of the direction of the ray at the boundary and the incident direction of the laser. If $P(\theta) = -1$, this ray satisfies the incident condition with regard to the direction. The solution of $P(\theta) + 1 = 0$ is obtained by the bisection method. Note that the iteration number of the bisection method means the number of the inverse ray trace calculation. Finally, whether or not this ray can intersect with the incident area is calculated. This procedure is one method by which to search for the exact ray that satisfies the incident condition.

In these consecutive procedures, geometrical effects like light focus are not considered. However, these geometrical effects can be reflected by adding a specific width to the ray. Therefore, subsidiary rays are introduced at each side of the ray and are also computed by ray tracing. Figure 4 illustrates the subsidiary rays with the main ray, where d_0 and d_1 are the distance of the two subsidiary rays at the incident area and the grid point, respectively. The ratio of d_0 to d_1 represents the degree of the light focus. The effect of the light focus is reflected by multiplying the intensity by this ratio.

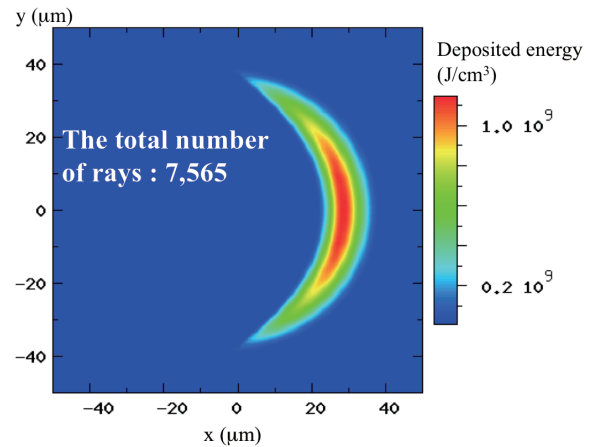


Fig. 5 The distribution of energy deposited on the same profile with Fig. 2 (a) by the use of the new algorithm.

Figure 5 shows the energy distribution deposited on the same plasma profile as in Fig. 2 (a) in the case of the new algorithm. A non-physical distribution as in Fig. 2 (b) does not occur and is similar to that in Fig. 2 (c). The total number of rays that just pass through each grid point is 7,565. The reason why that the total number differs from the total number of grid points is that there are no rays at grid points above the critical density. That multiple rays exist at some grid points as shown in Fig. 3 should also be considered. The total number of rays is less than that of the conventional result with 10,000 rays. However, the computational cost is approximately 20 times as great. This reason is that the iteration number at the stage of the bisection procedure is 10-20. This means that the inverse ray trace calculation is conducted 10-20 times at each grid.

There is room for improvement of the search algorithm to reduce the computational cost. On the other hand, this new algorithm does not generate the non-physical distribution associated with the number of rays and enables the calculation to be made only for necessary points.

4. Implosion Simulation

As a first step, we performed a preliminary three-dimensional implosion simulation by pressure drive instead of laser ablation, in which the non-uniformity due to the laser irradiation is reflected in the initial pressure profile. The initial pressure is defined from the laser absorption distribution. In this preliminary simulation, we used the previous result (Fig. 5) as assuming axial symmetry, where a geometrical effect for the axial symmetry is considered in the process of the focus factor. We define r_0 and r_1 as the distance between the axis and the ray position of the incident point and the distance between the ray position of the grid point and the axis. Then, the ratio of r_0 to r_1 is multiplied by the intensity. The energy distribution obtained from this process is integrated in the direction of the radius and normalized. This is defined as the distribution

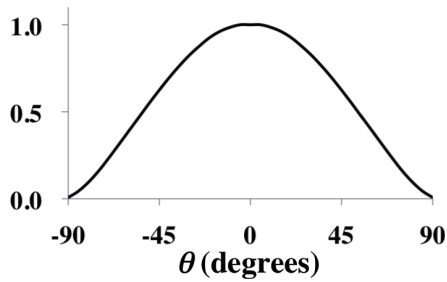


Fig. 6 The distribution function of the pressure perturbation by one laser beam. θ is the angle measured from the laser axis.

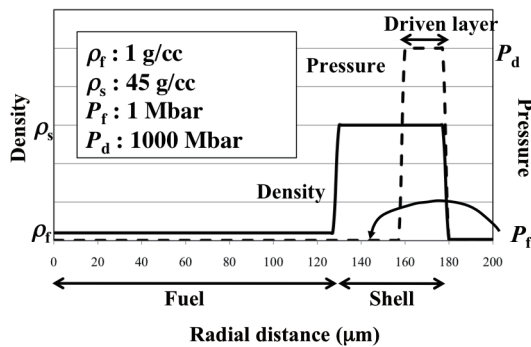


Fig. 7 The initial profile. The solid and dashed lines are the density and pressure, respectively. ρ_f and ρ_s denote the density of the fuel and shell. P_f and P_d are the pressure of the fuel and driven layer. The driven layer accelerates the target inward.

function for the pressure perturbation by one laser beam. Figure 6 shows the distribution function for the pressure perturbation by one laser beam. θ is the angle measured from the laser axis.

To simulate the implosion, a pure three-dimensional hydro code, IMPACT-3D [11], is used. IMPACT-3D solves compressible and inviscid hydro equations on Cartesian grids. The implosion target is assumed to be a spherical shell target and the initial condition is shown in Fig. 7, in which the “driven layer” generates the driving force for the target to accelerate inward. The pressure in the “driven layer” will be given the perturbation as the form of $P_d \times f(\theta)$, where $f(\theta)$ is the distribution function that is defined by one laser beam (see also Fig. 6). As for the irradiation orientation, GekkoXII at Osaka University is used. GekkoXII has twelve laser beams and is designed to be irradiated into a target with a dodecahedron orientation [12, 13]. Figure 8 shows the pressure profile of the “driven layer” as a result of overlapping twelve beams of GekkoXII.

Figure 9 shows the density iso-surface that corresponds to the fuel-shell interface near the maximum compression time. It has been found that the surface irregularity caused by GekkoXII irradiation orientation is enhanced by Rayleigh-Taylor instability. In the case of laser implosion, the target is consecutively accelerated inward during

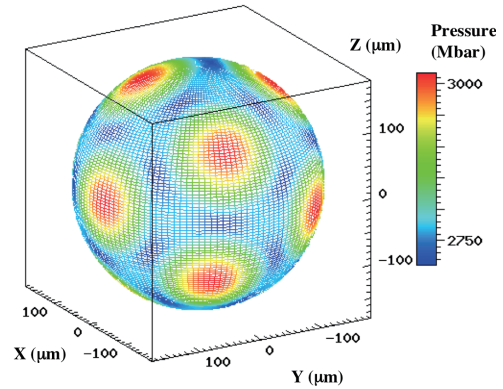


Fig. 8 Pressure profile of the driven layer.

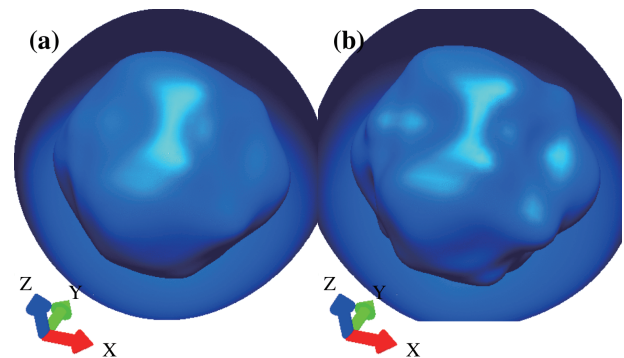


Fig. 9 The density iso-surface that corresponds to the fuel-shell interface. A maximum compression time of (a) 1.84 nsec and (b) 2.04 nsec.

irradiation by the laser. The surface irregularity caused by the orientation of the irradiation is emphasized more.

From this simulation result, it has been determined that the numerical perturbations that appeared in the conventional ray tracing calculation is a critical issue. Therefore, the new ray tracing method will be required. As a next step, we will introduce laser absorption into our hydro code and simulate the implosion by laser ablation.

- [1] S. Atzeni and J. Meyer-ter-Vehn, *The Physics of Inertial Fusion* (Clarendon Press, Oxford, 2004).
- [2] H. Takabe *et al.*, *Phys. Fluids* **28**, 3676 (1985).
- [3] F. Hattori *et al.*, *Phys. Fluids* **29**, 1719 (1986).
- [4] A. Casner *et al.*, *Phys. Plasmas* **19**, 082708 (2012).
- [5] H. Nagatomo *et al.*, *J. Plasmas Phys.* **72**, 791 (2006).
- [6] S. Atzeni, *Comput. Phys. Commun.* **43**, 107 (1986).
- [7] M. Temporal *et al.*, *Phys. Plasmas* **8**, 1363 (2001).
- [8] M. Temporal and B. Canaud, *Eur. Phys. J. D* **55**, 139 (2009).
- [9] A. Sunahara *et al.*, *Plasma Fusion Res.* **3**, 043 (2008).
- [10] R.S. Craxton and R.L. McCrory, *J. Appl. Phys* **56**, 108 (1984).
- [11] H. Sakagami and K. Nishihara, *Phys. Rev. Lett.* **65**, 432 (1990).
- [12] N. Miyanaga *et al.*, *Proceedings of 1st International Conference on Solid State Lasers for Application to Inertial Confinement Fusion*, CA, SPIE **2663**, 183 (1996).
- [13] M. Heya *et al.*, *Laser Part. Beams* **19**, 267 (2001).